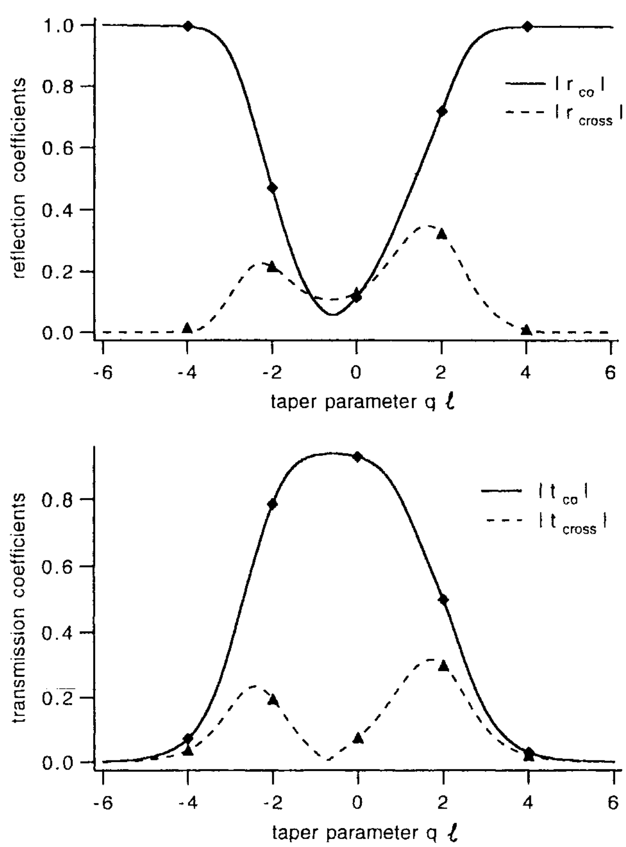

Fig. 2. The co- and cross-line reflection and transmission coefficients given by the explicit solutions (49) and (50) for two coupled identical exponential lines with the parameters $C_0 = C_{l0} = C_{00}$, $C_{m0} = 0.5C_{00}$, $L_0 = 3L_{00}$, $L_{l0} = 0.8L_{00}$, $L_{m0} = 2L_{00}$ and the frequency $\omega = 0.1/l\sqrt{L_{00}C_{00}}$. The marks in the figure are the corresponding co- and cross-line scattering coefficients obtained by solving numerically the ODE's for the reflection-coefficient matrix and the Green's functions.

V. Conclusion

The exact and explicit expressions for the co- and cross-line reflection and transmission coefficients for two coupled identical exponential lines have been derived. The explicit expressions have been validated by a numerical solution based on the wave-splitting technique.

References

[1] R. N. Ghose, "Exponential transmission lines as resonators and transformers," *IRE Trans. Microwave Theory Tech.,* vol. MTT-5, pp. 213–217, July 1957.

[2] C. P. Womack, "The use of exponential lines as microwave components," *IRE Trans. Microwave Theory Tech.,* vol. MTT-10, pp. 124–217, Mar. 1962.

[3] N. H. Younan, B. L. Cox, C. D. Taylor, and W. D. Prather, "An exponentially taped transmission line antenna," *IEEE Trans. Electromag. Compat.,* vol. 36, pp. 141–144, May 1994.

[4] S. He, "Closed-form solution for lossy exponential transmission line problem in frequency and time domains," *J. Electromag. Waves Appl.,* vol. 9, no. 4, pp. 521–540, 1995.

[5] G. Matthaei, L. Young, and E. M. T. Jones, *Microwave Filters, Impedance-Matching Networks, and Coupling Structures.* Norwood, MA: Artech House, 1980.

[6] J. R. Griffith and M. S. Nakhla, "Time-domain analysis of lossy coupled line system," *IEEE Trans. Microwave Theory Tech.,* vol. 38, pp. 1480–1487, Oct. 1990.

[7] C. E. Baum, "From the electromagnetic pulse to high-power electromagnetics," *Proc. IEEE,* vol. 80, pp. 789–817, June 1992.

[8] M. K. Krage and G. I. Haddad, "Characteristics of the coupled microstrip transmission lines-I: Coupled-mode formulation of inhomogeneous lines," *IEEE Trans. Microwave Theory Tech.,* vol. MTT-18, pp. 217–222, Apr. 1970.

[9] C. Nwoke, "An exact solution for the nonuniform transmission line problem," *IEEE Trans. Microwave Theory Tech.,* vol. 38, pp. 944–946, 1990.

[10] S. Amari, "Comments on an exact solution for nonuniform transmission line problem," *IEEE Trans. Microwave Theory Tech.,* vol. 39, pp. 611–612, Mar. 1991.

[11] J. L. Hill and D. Mathews, "Transient analysis of systems with exponential transmission lines," *IEEE Trans. Microwave Theory Tech.,* vol. MTT-25, pp. 777–783, Sept. 1977.

[12] J. K. Hale, *Ordinary Differential Equations.* New York: Wiley, 1969, pp. 93–100.

[13] S. He and S. Ström, "Time-domain wave-splitting approach to transmission along a nonuniform LCRG line," *J. Electromag. Waves Appl.,* vol. 6, no. 8, pp. 995–1014, 1992.

[14] S. He, "A time-harmonic Green's function technique and wave propagation in a stratified nonreciprocal chiral slab with multiple discontinuities," *J. Math. Phys.,* vol. 33, no. 12, pp. 4103–4110, 1992.

[15] R. P. Arnold, W. L. Bailey, and R. L. Vaitkus, "Normalized impedance graphs for exponential transmission line," *IEEE Trans. Microwave Theory Tech.,* vol. MTT-22, pp. 964–965, Nov. 1974.

Operation of New Type Field Displacement Isolator in Ridged Waveguide

Wen Junding, Wenquan Che, Yongzhong Xiong, and Yongwu Wen

***Abstract*—A new type ridged-waveguide field-displacement isolator is analyzed in this paper. Experimental results have been obtained for the isolation, insert loss, and voltage standing wave ratio (VSWR) in C- and X-band. The isolation and bandwidth are found to increase obviously.**

***Index Terms*—Isolator, ridged waveguide.**

I. Introduction

In 1960, Chen [1] proposed the experimental results of resonating isolator and field displacement isolator in a single ridged waveguide. He got useful results of the resonating isolator. As to the field displacement isolator, his experiments were failures. He found "the forward loss of the field displacement isolator in single ridged waveguide became nearly identical with the reverse loss, nonreciprocal effect was not distinct. Take out the resistance sheet, nonreciprocality couldn't be improved$\cdots$." Based on the study of [2]–[5], the authors think that Chen's failure is due to the asymmetry of the single ridge positioned in the waveguide, which caused asymmetrical field distribution, and to the spacing of the ridge from the ferrite, which was so far that the circular polarization field besides the ridge could not interfere with the magnetized ferrite. According to previous analysis, the authors propose a new type field displacement isolator in symmetrical ridged waveguide. The experimental work has shown

Manuscript received June 28, 1996; revised January 24, 1997.

The authors are with the Department of Electronical Engineering, Nanjing University of Science & Technology, Nanjing, 210094 R.O.C.

Publisher Item Identifier S 0018-9480(97)02900-1.

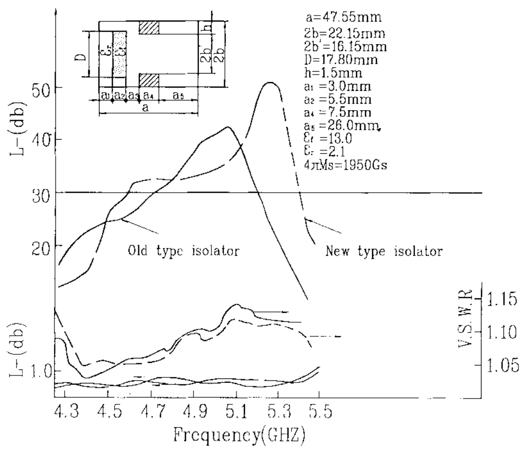

Fig. 1. Measured operation of new type field displacement isolator in ridged waveguide and old type isolator in rectangular wavegide in C-band.

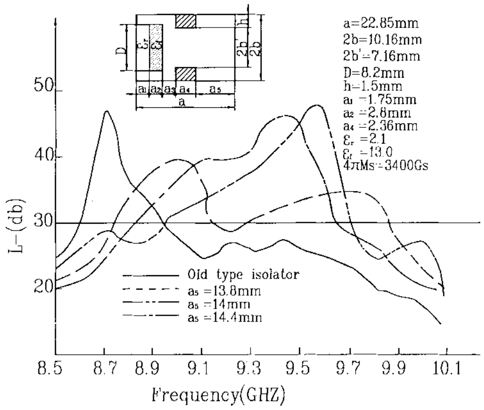

Fig. 2. Measured operation of new type field displacement isolator in ridged waveguide and old type isolator in rectangular waveguide in X-band.

that isolation and the bandwidth of the new type device have been improved.

II. Experimental Results

For the sake of the study, the authors use the ridged waveguide to replace the rectangular one, and do some experiments as following. In C-band, the length of the ferrite bar is 118.5 mm, the experimental results are shown in Fig. 1, where it can be seen that: 1) when the isolation $L-$ is 30 dB, the bandwidth of the new type device is 14.73%, while that of the old type devise is 9.7%; 2) the maximum isolation of the new type device is $7 \sim 8$ dB larger than that of the old type devise; and 3) the forward loss $L+$ of the new type device is slightly larger than that of the old type devise. In X-band, the length of the ferrite bar is 37.5 mm, with the experimental results shown in Fig. 2. One can see that the isolation of the new type device is larger than that of the old type devise. The experimental results have also shown that the forward loss of the new type device is larger slightly than that of the old type devise.

III. Theoretical Consideration

Since the ferrite and dielectric slabs loaded into the field displacement isolator are not "full height," it would be very difficult to get a closed form solution. In order to verify the isolation increase of the new type device, the authors draw in the analytical model [7] shown in Fig. 3, and use the transverse matrix method [3] to deduce the

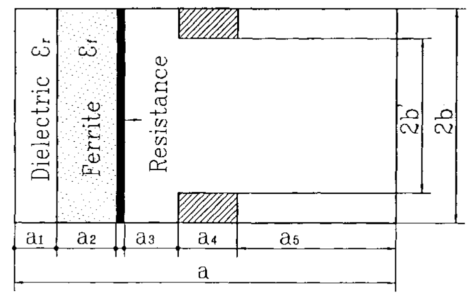

Fig. 3. Analytical model.

transcendental equation of the field displacement isolator in ridged waveguide as following:

$$j(A+B/Z)(tg\Phi+\xi tg\theta-vtg\theta tg\Phi) - B(1+v^2)tg\theta tg\Phi/\xi+B(1+vtg\theta)=0 \tag{1}$$

where

$$A = 1+j2Y_1tg\Phi_1-\left(\frac{b}{b},+Y_1^2\frac{b'}{b}\right)tg\Phi_1tg\Phi_2+jY_1\frac{b'}{b}tg\Phi_2 - \frac{'}{b}tg\Phi_2tg\varphi_3-jY_1\frac{b'}{b}tg\Phi_1tg\Phi_2tg\Phi_3-tg\Phi_1tg\Phi_3$$

$$B = jtg\Phi_1+j\frac{b'}{b}tg\Phi_2+jtg\Phi_3-2Y_1tg\Phi_1tg\Phi_3 - j\left(\frac{b}{b'}+Y_1^2\frac{b'}{b}\right)\cdot tg\Phi_1tg\Phi_2tg\Phi_3 - Y_1\frac{b'}{b}tg\Phi_2tg\Phi_3-\frac{b'}{b}Y_1tg\Phi_1tg\Phi_2$$

$$\Phi_1 = k_aa_5, \qquad \Phi_2 = k_aa_4, \qquad \Phi_3 = k_aa_3,$$

$$\theta = k_ma_2, \qquad \Phi = k_ca_1$$

$$k_a = \sqrt{\frac{\omega^2}{C^2}+\Gamma^2}$$

$$k_m = \sqrt{\frac{\omega^2}{C^2}\epsilon_f\mu_e+\Gamma^2}$$

$$k_c = \sqrt{\frac{\omega^2}{C^2}\epsilon_r+\Gamma^2}$$

$$v = -\frac{jk\Gamma}{\mu k_m}$$

$$\xi = \frac{k_a}{k_m}\frac{\mu^2-k^2}{\mu}$$

$$Z = \frac{R_sk_a}{\omega\mu_0}$$

$$Y_1 = j2b\omega C_d$$

C the light speed

C_d see [8], references herein.

Calculation parameters are given in the experimental results. The frequency range is from 8.0 to 11.0 GHz. The theoretical results are shown in the plots of Fig. 4, where it can be seen that the isolation of the new type device is about 3 dB larger than that of the old type one, which is roughly consistent with the experimental results shown is Fig. 2. The calculation has also shown that the isolation of the new type device reach its maximum value at $a_4 = 2.5$ mm, which agree with the experimental results shown in Fig. 2.

IV. Conclusion

In this paper, how to improve the isolation and bandwidth of the field displacement isolator in rectangular waveguide has been

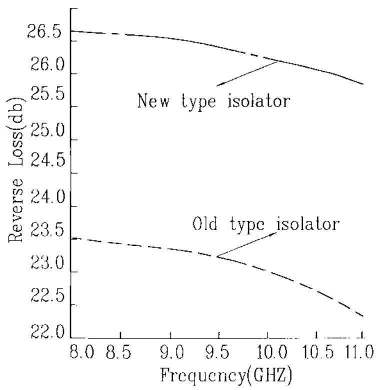

Fig. 4. Calculated reverse loss with frequency for new type isolator and old type isolator in X-band.

considered. The propagation constant transcendental equation has been deduced. By using appropriate ridged waveguide instead of rectangular one, it is possible to increase the isolation and bandwidth of the field displacement isolator, thus making it easier to get a good match. However, the forward insert loss of the new type device is slightly larger than that of the old type devise, and how to reduce the forward loss is of further work. The authors believe that this paper has resulted in a sufficient amount of knowledge regarding the device and provides a quantitative guide to the design of microwave devices.

References

[1] T. S. Chen, "Nonreciprocal attenuation of ferrite in single ridge waveguide," *IRE Trans. Microwave Theory Tech.*, vol. MTT-48, pp. 247–248, May 1960.

[2] W. Junding, "Analysis of transverse magnetization phase shifter of cross waveguide," in *Nat. Interchange Conf. Magnetic Material, Device Tech.*, Guanxian, Sichuan, China, Oct. 1977, pp. 1–8.

[3] ——, "Experimental studies of latching ferrite phase shifter of back ridged waveguide," *Acta. Electron. Sin.*, no. 3, pp. 44–51, Sept. 1979.

[4] W. Junding, Y. Z. Xiong, M. J. Shi, G. F. Cheng, and M. D. Zu, "Analysis of twin ferrite toroidal phase shifter in grooved waveguide," *IEEE Trans. Microwave Theory Tech.*, vol. 42, pp. 616–621, Apr. 1994.

[5] Y. S. Xu, "Microwave ferrite toroidal phase shifter in grooved waveguide with reduced sizes," *IEEE Trans. Microwave Theory Tech.*, vol. 36, pp. 1095–1097, June 1988.

[6] A. Mizobuchi and W. Kwrebagashi, "Nonreciprocal remanence ferrite phase shifter using the grooved waveguide," *IEEE Trans. Microwave Theory Tech.*, vol. MTT-26, pp. 1012–1017, Dec. 1978.

[7] R. L. Comstock and C. E. Fay, "Operation of the field displacement isolator in rectangular waveguide," *IEEE Trans. Microwave Theory Tech.*, vol. MTT-8, pp. 605–611, Nov. 1960.

[8] I. R. Whinery and H. W. Jamieson, *Proc. IRE*, vol. 32, pp. 98–115, Feb. 1944.

An Accurately Scaled Small-Signal Model for Interdigitated Power P-HEMT up to 50 GHz

Shen-Whan Chen, Olaleye Aina, Weiqi Li, Lee Phelps, and Tim Lee

***Abstract*—In this paper, the authors report an approach for constructing scalable small-signal models for interdigitated power pseudomorphic high-electron-mobility transistors (P-HEMT's). By using cold-FET and Yang–Long measurement, as well as direct extraction procedures, scaling rules for extrinsic components were established that allow accurate models over a broad frequency range. These models have been used to design ultrawide-band monolithic microwave integrated circuits (MMIC's) up to 50 GHz.**

I. Introduction

Small-signal equivalent models are used frequently in the design of power amplifier (PA), low-noise amplifier (LNA), and other subsystem components. A small-signal model which provides good accuracy and can be scaled based on layout structures, as well as gatewidth, is useful when various FET sizes are needed or models are simply not available. Unlike the small-signal model that is determined by computer optimization, a physically related one can be useful in the characterization of fabrication processes and for scaling purposes. In addition to providing an equivalent circuit to predict MMIC electrical performance, a scalable modeling approach is also useful in determining the noise parameters [1]–[2]. In this paper, an approach to constructing a scalable small-signal model from cold-FET, Yang–Long measurement, and RF data for an interdigitated power pseudomorphic high-electron-mobility transistor (P-HEMT) is presented. Approaches for selecting the parameters from data sets are discussed. The scaling factors for extrinsic components (R_g, R_d, R_s, L_g, L_d, L_s, $C_{\rm pg}$, and $C_{\rm pd}$) are given after careful examination of the measured data. The S-parameter comparison between scaled models and measured data are shown up to 50 GHz.

II. Power P-HEMT Device Structure and Equivalent Circuit

The pseudomorphic InGaAs/AlGaAs HEMT device structure was used in this paper. The device profile is a double-heterojunction HEMT grown by molecular beam epitaxy (MBE). Silicon planar doping is employed on both heterojunctions to provide carriers to the InGaAs channel. The AlGaAs layer with the planar doping was left undoped and the Schottky gate was recessed to this region. Ohmic contacts were formed with an optimized rapid thermal annealing (RTA) AuGeNi-based metallization scheme. Device isolation was achieved by boron ion implantation. The devices were passivated with SiN film deposited by plasma-enhanced chemical-vapor deposition (PECVD). Due to the use of undoped AlGaAs, the gate–drain breakdown voltage (defined at 1 mA/mm) is greater than 12 V.

Fig. 1 shows the chosen equivalent circuit topology for the interdigitated power P-HEMT. The P-HEMT layout in wafer process control monitored (PCM) sites is shown in Fig. 2. The S-parameters of five different FET's, 100 μm (25 $\times$ 4, two gate feeds), 198 μm (33 $\times$ 6, three gate feeds), 300 μm (30 $\times$ 10, five gate feeds), 396 μm (33 $\times$ 12, six gate feeds), and 600 μm (50 $\times$ 12, six gate feeds) are measured and their small-signal models are extracted with methods discussed below.

Manuscript received July 24, 1996; revised January 24, 1997.

The authors are with the M/A-COM, IC Business Unit, Millimeter IC Product, Clarksburg, MD 20871 USA.

Publisher Item Identifier S 0018-9480(97)02904-9.